High Voltage

Research Article

IET Journals
The Institution of Engineering and Technology

# Comparative study on various dielectric barriers and their effect on breakdown voltage

ISSN 2397-7264
Received on 13th March 2017
Revised 6th October 2017
Accepted on 17th October 2017
E-First on 8th November 2017
doi: 10.1049/hve.2017.0032
www.ietdl.org

*Elham Foruzan*[1] ✉, *Amir A.S. Akmal*[2], *Kaveh Niayesh*[3], *Jeremy Lin*[4], *Desh Deepak Sharma*[5]

[1]*Department of Electrical and Computer Engineering, University of Nebraska-Lincoln, Lincoln, NE 68588, USA*
[2]*Department of Electrical and Computer Engineering, University of Tehran, Tehran, Iran*
[3]*Department of Electric Power Engineering, Norwegian University of Science and Technology, Trondheim, Norway*
[4]*PJM Interconnection, Audubon, PA 19403, USA*
[5]*Department of Electrical Engineering, MJP Rohilkhand University, Bareilly (UP), India*
✉ *E-mail: elham.foruzan@huskers.unl.edu*

**Abstract:** Non-pressurised air is extensively used as basic insulation medium in high-voltage equipment. Unfortunately, an inherent property of air-insulated design is that the system tends to become physically large. On the other hand, the application of dielectric barriers can increase the breakdown voltage and therefore decrease the size of the equipment. In this study, the impact of dielectric barriers on breakdown voltage enhancement is investigated under both direct current (dc) and alternating current (ac) applied voltages. For this purpose, three kinds of dielectric barriers in two different high-voltage electrode structures are investigated. In the first structure, several experiments are carried out with four different electrode arrangements, keeping the inter-electrode gap constant while varying the position of the dielectric barrier between the electrodes. In the second structure, the inter-electrode gap is varied while the high-voltage electrode is covered with dielectric materials. The influences of different parameters such as inter-electrode spacing, electric field non-uniformity factor, and dielectric materials on the breakdown voltage are investigated for applied 50 Hz ac and dc voltages. In addition, a simulation model to approximately calculate the breakdown voltage is proposed and validated with the experimental results.

## 1 Introduction

In gas-insulated high-voltage (HV) systems, non-pressurised air is mainly used as the basic insulation medium. However, the air-insulated designs are physically large. On the other hand, an alternative to non-pressurised air is sulphur-hexafluoride ($SF_6$), which is an organic, colourless, and odourless gas that has higher dielectric strength than air [1]. This property can significantly reduce the size of HV systems. However, the application of $SF_6$ and its mixtures in HV systems will decline in the future due to the certain drawbacks such as environmental considerations, complex construction, and complicated maintenance.

Dielectric barriers in air-insulated systems have been considered as a possible replacement for $SF_6$ [1–3]. The application of dielectric barriers in the HV systems brings the beneficial use of surface charges on the barrier to improve the breakdown performance of air-insulated systems [4–6]. Charge accumulation on the dielectric barrier surface reduces the electric field at the location of a micro-discharge, which results in current termination [7–12]. Furthermore, redistribution of the electric field in the air gap, due to accumulated surface charges on the dielectric barrier, affects the breakdown voltage of the gap. These surface charges are the result of impact ionisation near the HV electrode. In [13–15], a charge simulation technique was used to investigate the breakdown voltage and electric field in needle/plane electrodes while one of electrodes was coated with a dielectric barrier. Blennow and Sjoberg [4] presented a model for describing a uniform electric field distribution in a plate–plate electrode configuration where the ground plate was covered by a dielectric layer. They showed that the surface charges over the barrier decrease the electric field in the air gap and increase the breakdown voltage. Vogelsang *et al.* [16] inserted a mica-epoxy insulator between two electrodes to slow down tree propagation. In their experiment, they applied a constant HV to the electrodes and measured the time to formation of a complete breakdown discharge (measuring electrical tree propagation) – this time to complete discharge formation is defined as the 'breakdown time'. Inserting a dielectric barrier significantly increased the breakdown time. In [17], the effect of the surface charges deposited on the Pyrex dielectric was investigated in a point-to-plane geometry with the dielectric covering the plane electrode. They found that these surface charges have a strong impact on the discharge structure. Polymeric and cellulose materials are widely used as HV insulation materials. Although several studies explored the insulating performance of polymeric materials, there are many obstacles for using these materials in HV applications due to lack of understanding of their behaviour and performance in the presence of surface charges [18].

To better understand the effect of polymeric and cellulose materials as barriers in HV systems, two different studies were conducted in this paper. In the first case study, we investigate the effect of positioning polytetrafluoroethylene (PTFE) and cellulose dielectric barriers between two electrodes in semi-uniform and non-uniform electric field distributions, shown schematically in Fig. 1*a*. Furthermore, a study was performed to compare the effect of different thicknesses of these two dielectric materials to further explore their performance in HV systems. In the second case study, an HV electrode was covered with three different thicknesses of polymeric dielectric barrier. The impact of the non-uniformity factor of the electric field as well as the influence of the dielectric material characteristics are investigated.

Additionally, simulation models with the presence of a barrier for the pre-breakdown instant were developed based on finite-element method and using COMSOL Multiphysics. The simulation results were verified with the experimental results obtained in the laboratory to validate the accuracy of the models.

## 2 Experimental setup

In this section, we present two case studies for two different electrode structures in the presence of a dielectric barrier. The experimental setup is then described.

In the first structure, a dielectric barrier was inserted into an inter-electrode air gap for four different electrode geometries listed as follows:

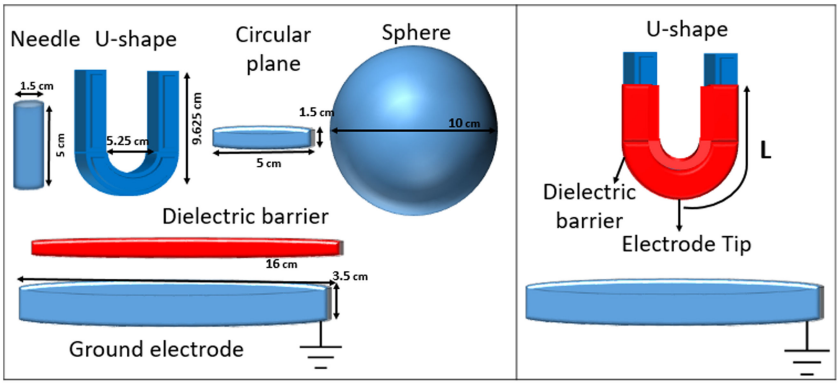


**Fig. 1** *Schematic diagrams for two different electrode structures in the presence of a dielectric barrier*
***(a)*** Four electrode geometries studied in semi-uniform and non-uniform fields, ***(b)*** U-shape electrode with dielectric coating used to investigate non-uniformity and materials effects

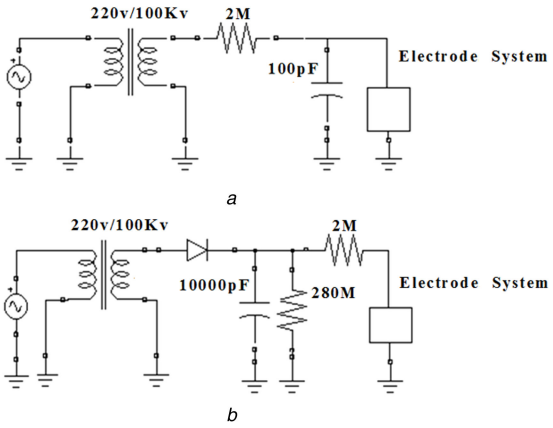


**Fig. 2** *Schematic diagram for the experimental system for*
***(a)*** ac voltage, ***(b)*** dc voltage

i. Needle/plane
ii. U-shape/plane
iii. Plane/plane
iv. Sphere/plane

Fig. 1*a* shows the schematic diagram for the four electrode geometries. The four different electrode geometries in the first case study are used to investigate the effect of adding dielectric barrier in different electric field distributions. The electric field distribution between needle/plane and U-shape/plane electrodes is non-uniform, while the electric field distribution in the plane/plane and sphere/plane electrode systems is more uniform, and we consider them to have 'semi-uniform' electric field distributions.

In the set of experiments, a dielectric barrier was parallel with the grounded plane electrode and its distance from the grounded electrode was vertically changed while the inter-electrode distance was kept constant. In these set of experiments, two different thicknesses of PTFE, 0.2 and 1 mm, and three different thicknesses of pressboard, including 0.2, 0.4, and 1 mm were used. Also, dielectric barriers were 16 cm diameter circular shapes in this set of experiment.

In the second structure, a U-shape HV electrode was covered with polyvinyl chloride (PVC) as a dielectric barrier. Fig. 1*b* shows the schematic diagram for U-shape electrode coated with PVC dielectric barrier, which are created in the laboratory. We made 1000 U-shape electrodes using 2.6 mm copper wire in the laboratory for a set of experiments, since in each experiment the applied voltage was increased until the HV electrode was punch. To create samples, first, a 5.25 cm diameter curvature was created to produce a U-curvature shape in the electrode and then, the 7 cm vertical heights of left- and right arms of the U-shape electrode were created. The ground electrode was a stainless steel, circular plane electrode with a 16 cm diameter as can be seen in Fig. 1. In this case study, the breakdown voltages were studied for both 0.32 and 0.64 mm thicknesses of PVC barrier coatings. Experiments were also carried out for four different inter-electrode distances. The geometric dimensions of all electrodes are shown in Table 1 and Fig. 1. The properties of the dielectric materials are listed in Table 2.

**Table 1** Geometric dimensions of electrodes

| Electrode | Shape | Diameter, cm | Height, cm |
|---|---|---|---|
| needle | cylinder | 1.5 | 5 |
| U-shape electrode | U-shape | 5.25 | 9.625 |
| plane | circular | 5 | 1.5 |
| grounded plane | circular | 16 | 3.5 |
| sphere | sphere | 10 | — |

**Table 2** Properties of dielectric materials used in experiments

| | Relative permittivity ($\epsilon_r$) | Dielectric strength, kV/mm |
|---|---|---|
| PVC | 2.5 | 20 |
| PTFE | 2.1 | 60 |
| pressboard | 3 | 16 |

Fig. 2 shows the experimental setup for alternating current (ac) and direct current (dc) voltages. The HV electrode connects to a 220 V/100 kV HV transformer through one 2 MΩ resistor that controls current while the lower plane electrode is grounded. Applied voltage across the electrode system was measured by a capacitive voltage divider consisting of two discharge-free vacuum capacitors. Voltage across the electrode system was gradually increased with the constant rate of 2 kV/s until the breakdown between electrodes occurred.

## 3 Simulation modelling

The influence of a dielectric barrier on the electric field and voltage distribution was analysed using COMSOL Multiphysics software, which is based on finite-element method [19, 20]. In these models, the pre-breakdown instant was simulated in the ac/dc module of COMSOL Multiphysics.

To find the electric field and voltage distribution, first each system geometry was plotted in the computational domain. Boundary conditions including surface charge distribution, material properties, and applied voltage to HV electrodes were entered into the simulation model. The boundary conditions used in the simulation are described in the following section. Then, electric field and voltage distributions in the air gap are calculated using *Laplace's equation*

$$-\nabla^2(\epsilon \cdot V) = 0, \quad E = -\nabla V, \tag{1}$$

where $E$ and $V$ are the electric field and potential, respectively, and $\epsilon$ is the permittivity coefficient.

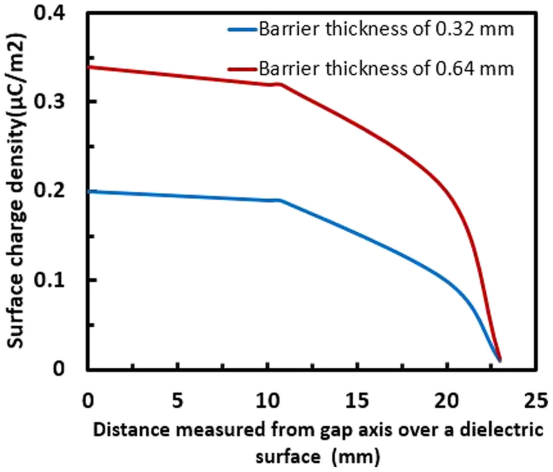


**Fig. 3** *Surface charge density on the U-shape dielectric structure as a function of the distance from the electrode tip (noted in Fig. 1b)*

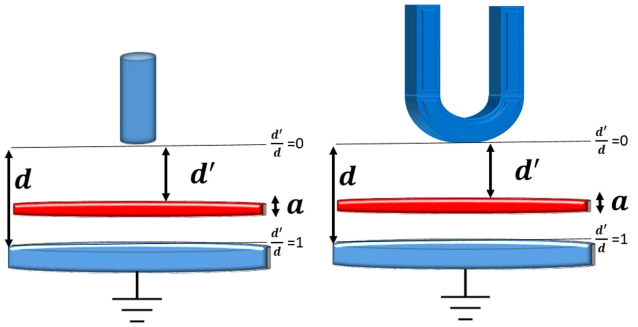


**Fig. 4** *Schematic diagram for needle/plane and U-shape/plane electrode geometries. These geometries are used to study the effects of a dielectric barrier in non-uniform electric field configurations*

### *3.1 Boundary conditions*

There are free charges in the air gap, available from field dependent and independent processes, such as micro-discharge and natural ionisation, respectively [4], and should be entered in the model as the initial condition. These free charges in the air gap are accumulated over the barrier surface due to electrostatic attraction, and later change the electric field distribution.

In the first structure, the dielectric barrier was inserted in the air gap between two electrodes. In this structure, the surface charge density on the dielectric barrier was assumed to have a bell shape, and was represented with a Gaussian distribution [17, 21, 22]

$$\sigma_s = \frac{Q_T}{2\pi\sigma^2} \mathrm{e}^{-r^2/2\sigma^2}, \tag{2}$$

where $\sigma$ is the mean impact radius of the charge deposited over the barrier and $r$ is the radius of the dielectric barrier; here, assumed to be equal to the dielectric radius. $Q_T$ is the maximum surface charge, which was varied in the range between 40 and 100 nC [17, 21, 22].

Fig. 3 shows the surface charge density calculated in COMSOL Multiphysics when the U-shape electrode was coated with a PVC dielectric barrier in the second structure. The surface charge density in this case was assumed to have a bell shape distribution for two different thicknesses of the dielectric barrier [23]. Longer flux lines result in a smaller amount of charge residue over the barrier, therefore, as can be seen in Fig. 3, the charge density decreases as $l$ increases, where $l$ is the distance from electrode tip along the dielectric length (noted in Fig. 1). In other words, the dielectric coated U-shape electrode has the maximum surface charge density at the electrode tip, and it decreases as the distance from electrode tip increases. The amount of surface charge for a 5 mm inter-electrode gap in two different barrier thicknesses was approximated according to the experimental results, and we applied the same distributions for other inter-electrode air gaps. Nevertheless, by increasing the inter-electrode gap from 5 to 30 mm, the amount of surface charges over the barrier was decreased.

### *3.2 Breakdown criteria*

The streamer breakdown criterion is considered for calculating the breakdown voltage in the simulation models. The streamer breakdown mechanism, formulated by Raether (1964) and Meek (1940), postulates that if the avalanche size grows to such an extent that space charge electric fields can be on the order of breakdown fields, then breakdown can proceed by the development of positive and negative streamers, driven by the space-charge fields. This criterion can be formulated as follows [24–28]:

$$\mathrm{e}^{\int_0^d (\alpha-\eta)} \geq Q, \tag{3}$$

where $\eta$ is the recombination coefficient, $\alpha$ is the ionisation coefficient, $d$ is gap distance, and $Q$ is a constant number. The values of $Q$ obtained by Raether (1964, p. 133) and Meek (1940), for streamer breakdown, are both on the order of $10^8$. Both the ionisation and recombination coefficients are functions of the electrical field and pressure as follows [29]:

$$\alpha = A \cdot p \cdot \mathrm{e}^{(-Bp/|E|)}, \quad \eta = A_1 \cdot p \cdot \mathrm{e}^{(-B_1 p/|E|)}, \tag{4}$$

where $A = 3.75 \times 10^5$, $B = 1.75 \times 10^7$, $A_1 = 0.016 \times 10^5$, and $B_1 = 0.265 \times 10^7$ for air.

In this study, the electric field distribution within the air gap of two electrodes with the presence of a dielectric barrier is numerically calculated by using COMSOL Multiphysics and Matlab softwares.

## 4 Results

Two sets of experimental and simulation results for two case studies are summarised in this section. First, the impact of inserting a dielectric barrier between electrodes was investigated. Next, the impact of coating U-shape electrode with PVC dielectric barriers was analysed.

### *4.1 Case study 1: effect of inserting dielectric barrier between electrodes*

Dielectric materials (pressboard and PTFE) in a circular shape were inserted in the air gap of electrodes for four different electrode arrangements. In each arrangement, a dielectric barrier was parallel to the grounded plane and was vertically moved in the constant inter-electrode air gap. First, we studied the impact of dielectric on the non-uniform and semi-uniform electric fields. Then, we investigated the effect of PTFE dielectric thicknesses on breakdown voltage. Finally, the simulation results were presented.

*4.1.1 Effect of dielectric barrier on non-uniform electric field:* The schematic diagram for two structures of needle/plane and U-shape/plane electrode arrangements consists of a dielectric barrier with thickness of $a$ and is shown in Fig. 4.

In this diagram, $d'$ is the vertical distance between the dielectric barrier and the HV electrode (needle or U-shape electrode), and $d$ is the distance between two electrodes. Dielectrics with three different thicknesses ($a$ in Fig. 4) were used in these sets of experiments. In each experiment set, the position of dielectric barrier changed from $d' = 0$ to $d' = 30$ mm. Therefore, the breakdown voltages were measured while the fraction $d'/d$ varied from 0 to 1. The breakdown voltage for the U-shape/plane and the needle/plane arrangements without a dielectric barrier at 30 mm inter-electrode air gap was measured 30 and 27 kV, respectively. The breakdown voltages for two structures of needle/plane and U-shape/plane electrode arrangements with a pressboard dielectric barrier are shown in Fig. 5. In this figure, each experiment, to measure breakdown voltage, was repeated ten times and the average of *ten* measured values was reported as the breakdown

voltage. The variance for each breakdown voltage point was relatively uniform and small.

As can be seen in Fig. 5, a dielectric barrier's location plays an important role in the breakdown voltage. The maximum breakdown voltage was obtained $d'/d \sim 0.15 - 0.2$. When the barrier was placed at this position in the air gap, its potential was practically equal to the HV electrode. This equality results in a more uniform electric field between the barrier and the ground electrode, due to accumulative charges on the barrier surface [17]. In other words, the barrier effect is associated with the redistribution of the electric field in the gap as a result of the ionisation near the HV electrode and the accumulating electric charges on the barrier surface. If the barrier is placed close to the HV electrode ($d'/d < 0.1$), then discharges are quite short and the accumulated charges on the barrier are not sufficient to change the uniform electric field of the barrier-plane gap. Therefore, the electric field of the whole arrangement remains non-uniform. Also according to the results, a thicker barrier has a significant impact on increasing the breakdown voltage; by increasing the dielectric thickness from 0.2 to 1 mm, the breakdown voltage was increased from 56 to 65 kV in the U-shape/plane electrode.

*4.1.2 Effect of dielectric barrier on semi-uniform electric field:* The schematic diagram for plane/plane and sphere/plane electrode arrangements with the presence of a dielectric barrier between the HV and ground electrodes is shown in Fig. 6. Again, $d'$ is the distance between the dielectric and the HV electrode (plane or sphere electrode) and $d$ is the distance between two electrodes. Again, the fraction $d'/d$ varied from 0 to 1. However, the distance between the two electrodes is set to 20 mm in this set of experiments; consequently, the distance from the dielectric barrier to the HV electrode, $d'$, ranges from zero to 20 mm.

Three different thicknesses of pressboard were used as dielectric barriers. In one case, the HV electrode was a plane with a 5 cm diameter and the grounded electrode was a 16 cm diameter plane. Therefore, the plane/plane electric field is not completely uniform but is relatively uniform compared to the U-shape/plane and needle/plane electrode arrangements. The breakdown voltages of the plane/plane and sphere/plane electrode arrangements without the dielectric barrier in a 20 mm inter-electrode air gap were measured to be 40 and 43 kV, respectively.

Breakdown voltages for plane/plane and sphere/plane electrode arrangements under dc voltage are shown in Figs. 7*a* and *b*, respectively.

Fig. 7*a* shows that the optimal position of the barrier in the plane/plane arrangement is approximately in the middle of the inter-electrode gap for all three different thicknesses. The optimum position of the barrier is defined as the location of the barrier in which the breakdown voltage is maximum. As shown in Fig. 7*a*, inserting a barrier in the air gap of the plane/plane electrodes results in $\simeq$ 40% increase in the breakdown voltage.

As can be seen in Fig. 7*b*, the breakdown voltage has a minimum point in the sphere/plane electrode arrangement. If the barrier is placed close to the ground electrode, the uniform electric field between the barrier and the grounded plane becomes so small that the barrier barely influences the whole gap. Therefore, the electric field remains semi-uniform. On the other hand, when the barrier covers the grounded plane electrode, it will prevent the streamer from reaching the plane, which increased the breakdown voltage [30]. When the barrier is close to either the HV or the ground electrodes, the breakdown voltage in the sphere/plane arrangement is higher compared with the plane/plane system. In those cases, the electric field of unequal diameter electrodes in the plane/plane arrangement is more heterogeneous than the sphere/plane electric field.

*4.1.3 Comparing dielectric barrier impact for the four electrode geometries:* In the U-shape/plane and needle/plane arrangements, the pressboard dielectric barrier increased the breakdown voltage up to 60 kV (Fig. 5), i.e. up to a factor of 2. However, inserting a barrier in the air gap of the plane/plane electrodes results in a <40% increase in the breakdown voltage.

A comparison of the results for plane (semi-uniform fields) and U-shape (non-uniform fields) electrodes shows that the effect of the barrier on increasing breakdown voltage in the non-uniform electric fields is more significant. The reason can be attributed to the non-uniformity factor, which quantifies the degree of non-uniformity associated with the electrode arrangement. The electric field non-uniformity is defined as the maximum electric field intensity in the gap, which occurs near the tip of the HV electrode, divided by the average electric field intensity [31]. Polarisation and corona appear much less in electric field configurations with a lower non-uniformity factor, as is the case with the plane electrode. The impact of the barrier is reduced because accumulated charges on the dielectric surface do not significantly influence the relatively homogeneous electric fields. The high intrinsic non-uniformity factor of the U-shape electrode means the dielectric barrier can significantly influence breakdown characteristics by effectively reducing the non-uniformity factor.

*4.1.4 Effect of PTFE as a dielectric barrier:* The effect of PTFE for two different thicknesses (0.2 and 1 mm) was investigated in four different electrode arrangements, namely: sphere, U-shape, needle, and plane electrodes. In all arrangements, the ground electrode was a 16 cm diameter plane electrode. Fig. 8 shows the results of breakdown voltage in these four arrangements.

Using a PTFE dielectric barrier, the peak breakdown voltage in both U-shape and needle electrode arrangements at $d'/d \sim 0.2 - 0.4$ is roughly two times higher than the minimum breakdown voltage in these configurations. However, as we mentioned earlier, the breakdown voltage slightly changed when a barrier was inserted close to the grounded plane ($d'/d \sim 0.85 - 1$). On the other hand, the experimental results obtained in Fig. 8 show that increasing the PTFE barrier thickness from 0.2 to 1 mm leads to more than two times increase in breakdown voltage in the area of $d'/d < 0.75$ and for all four electrode arrangements.

By comparing results of two dielectric thickness in Fig. 8, we can observe that when the PTFE barrier with 1 mm thickness was placed between needle/plane, U-shape/plane, and plan/plane electrode geometries, regardless of where it was placed in $d'/d < 0.75$, the maximum breakdown voltage has a variation <30%. However, PTFE with 0.2 mm thickness in these three electrode geometries is more sensitive to barrier location, i.e. $d'$. One probable reason is that the PTFE with 1 mm thickness has a high dielectric strength. Therefore, more charges (resulting from the discharge in the air gap) are accumulated over the barrier surface with respect to the 0.2 mm PTFE. With increasing external voltage, discharges occur when the electric field in the air gap exceeds its maximum field strength, causing more of these charges to accumulate on the barrier surface. They induce an electric field directly opposite to the applied electric field in the gap, leading to a rapid decrease in the consequent total electric field in the gap. A reduction of the electric field results in extinguishing of micro-discharges and breakdown voltage enhancement [17]. Also one can observe that the barrier effect is less pronounced at $d'/d > 0.75$. At these places, the effect of the dielectric barrier suddenly decreased in the air gap for all four electrode arrangements. This might happen because when the dielectric barrier comes very close to the ground electrode ($d'/d > 0.75$), the electric field caused by the residual surface charges over the barrier are so small that it cannot change neither the electric field distribution in the air gap between barrier and grounded electrode nor the electric field distribution between HV electrode and barrier, thus resulting in a no or slight changes in the breakdown voltage.

Also one more observation from Figs. 5 and 8 shows that the breakdown voltages for structures including PTFE are 50% higher than that for structures with the pressboard dielectric barrier in optimal dielectric locations. In the plane/plane arrangement, the PTFE dielectric barrier leads to an increase in the breakdown voltage from 40 to 64 kV in the optimal barrier location. On the other hand, the breakdown voltage for the same arrangement with the pressboard dielectric barrier increased to only 46 kV.

In sum, we conclude that the breakdown voltage significantly increased in structures with PTFE compared with those with pressboard. Additionally, the thicker layer of the PTFE (i.e. 1 mm

thickness) resulted in a significant increase in the breakdown voltage regardless of the positions where the dielectric barriers are placed.

*4.1.5 Simulation results:* In this section, we present a simulation model to calculate the breakdown voltage. The simulated results are compared with the experimental results to assess the accuracy of the model.

In our model, the streamer breakdown criterion was applied to evaluate the breakdown voltage in the proposed electrode arrangements. In the first step, the initial guesses for voltage were approximated using experimental data and were imported to the software as an initial condition. The electric field distributions for the breakdown voltage path were calculated and evaluated according to the field streamer criterion. If the criterion was not met, the voltage was increased by 2 kV and the whole procedure was repeated. The lowest voltage that met the criterion was selected as the breakdown voltage. By applying this method, it is possible to estimate the breakdown voltage for different electrode systems.

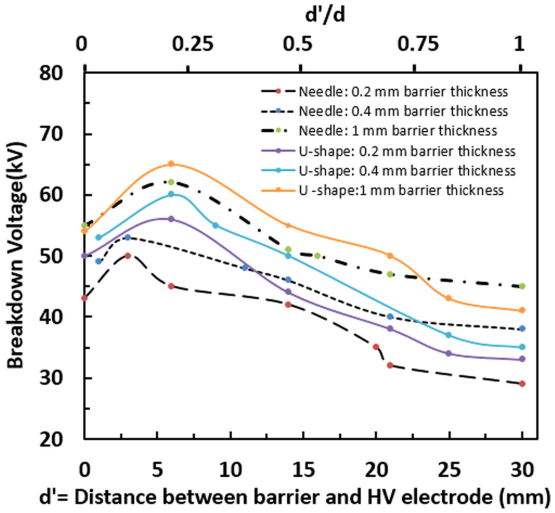


**Fig. 5** *Breakdown voltage of needle/plane and U-shape/plane arrangement under dc voltage, while the distance between the dielectric barrier and the HV electrode, d′, changes in a constant inter-electrode distance of d = 30 mm. A pressboard dielectric barrier is used in 0.2, 0.4, and 1 mm thicknesses*

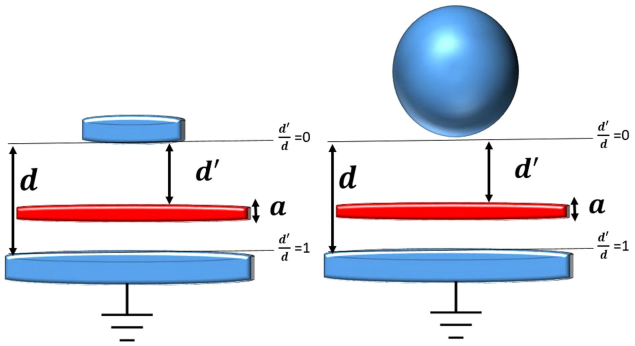


**Fig. 6** *Schematic diagram for the plane/plane and sphere/plane electrode geometries. These geometries are used to study the effects of a dielectric barrier in semi-uniform electric field configurations*

Here, we present the simulation results for two electrode arrangements, the needle/plane, as a representative for electrode with non-uniform electric field, and the sphere/plane, as a representative for an electrode with semi-uniform electric field. In each arrangement, four different locations of the dielectric barrier in the air gap were considered. Figs. 9 and 10 show the $y$–$z$ cross-section of the electric field distribution at the instant of pre-breakdown, for the needle/plane and sphere/plane electrode arrangements, respectively. These figures show the electric field distributions of the pre-breakdown instants for four dielectric barrier positions.

The simulation and experimental results of the breakdown voltage varying the location of dielectric barriers through the fixed inter-electrode gap are shown in Figs. 11 and 12. Fig. 11 shows the simulation and experimental results of the breakdown voltage in the needle/plane electrodes in the presence of a 1 mm pressboard dielectric barrier. We observe that both simulation and experimental results followed the same pattern. In both cases, the breakdown voltage increased when $d'/d$ increased from 0 to 0.15 and the maximum breakdown voltage occurred at $d'/d = 0.2$ mm. The breakdown voltage in both experiments and simulations decreased after $d'$ exceeds 6 mm, and minimum was reached when the barrier covers the ground electrode. For barrier positions at $d' = 20$ mm, the maximum deviation of the experimental and simulation results is around 25%.

The simulation and experimental breakdown voltages for the sphere/plane electrode configuration are shown in Fig. 12. The simulation results approximately align with the experimental breakdown voltages. As can be seen, when $d'$ is between 0 and 10 mm, the experimental results agree with the simulation results of the proposed model. For barrier positions bigger than 10 mm, the maximum deviation of the experimental and simulation results is around 20%. The unknown amount of $Q$ in (3) can be one reason for this error. The amount of $Q$ depends on the radius of the HV electrode, electric field uniformity, and other unknown parameters. Another interesting observation in Fig. 12 shows that experimental breakdown voltage in sphere/plane electrode configuration has a minimum value, which is not captured in the simulation. Unfortunately, a decisive reason to justify the minimum breakdown voltage in the experimental results is unknown.

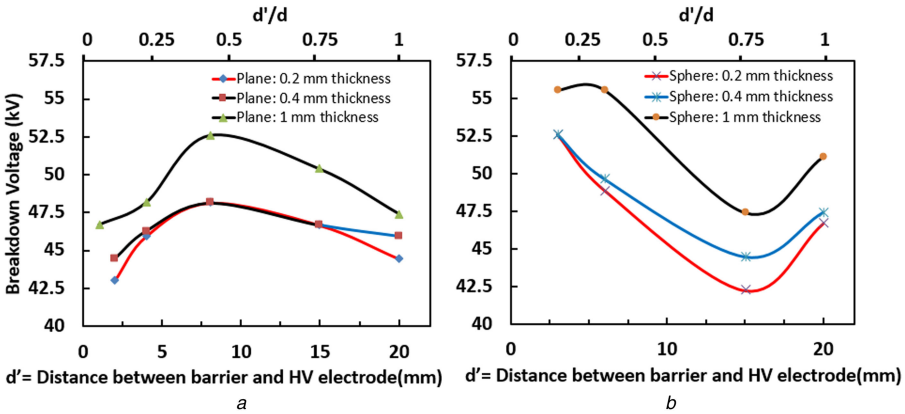


**Fig. 7** *Breakdown voltage of*

***(a)*** Plane/plane arrangement, ***(b)*** Sphere/plane arrangement under dc voltage, while the distance between barrier and the HV electrode, $d'$, changes in a constant inter-electrode distance of $d = 20$ mm

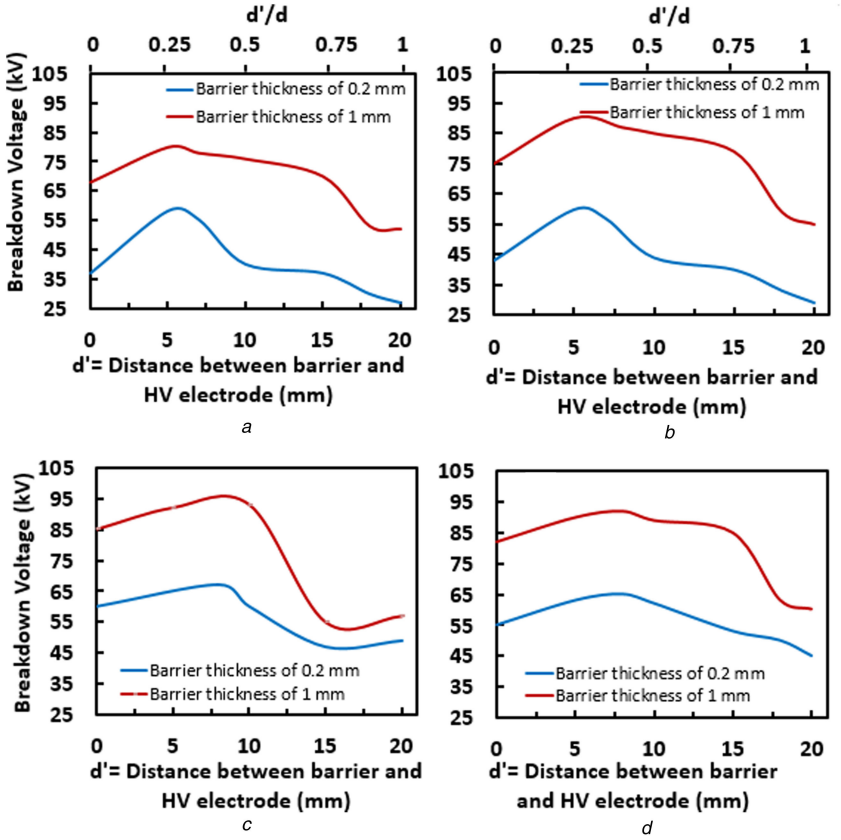


**Fig. 8** *Breakdown voltage for four different arrangements of*
***(a)*** Needle/plane, ***(b)*** U-shape/plane, ***(c)*** Sphere/plane, ***(d)*** Plane/plane under dc voltage with PTFE barrier. The distance between barrier and the HV electrode, $d'$, changes in a constant inter-electrode distance of $d = 20$ mm

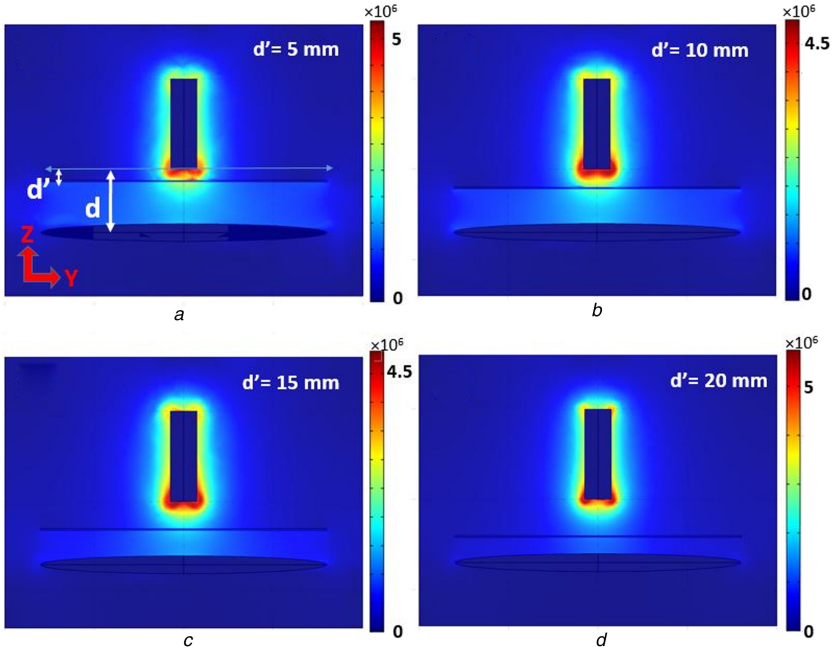


**Fig. 9** *Electric field distribution at pre-breakdown instant in needle/plane configurations in the presence of a dielectric barrier located at*
***(a)*** $d' = 5$ mm, ***(b)*** $d' = 10$ mm, ***(c)*** $d' = 15$ mm, ***(d)*** $d' = 20$ mm in a constant inter-electrode distance of $d = 30$ mm

### *4.2 Case study 2: the effect of coating the HV electrode with a dielectric barrier on the breakdown voltage*

In the second study, we covered the HV electrode with two different thicknesses of dielectric barriers and measured the breakdown voltage while the inter-electrode gap distance was varied. Each experiment was repeated ten times and the average of *ten* measured values was reported as the breakdown voltage. The variance for each breakdown voltage point was relatively small.

Fig. 13 shows the breakdown voltage versus the distance between electrodes under applied dc voltage. An increase of the inter-electrode gap enhances the breakdown voltage. Based on the results, the breakdown voltage for electrodes covered with the PVC were 3.43 times higher than the bare electrode at a 5 mm inter-electrode gap. This is because covering the electrode with a dielectric barrier reduces the maximum field intensity in the air gap due to residual surface charges over the dielectric barrier. The impact of the dielectric barrier saturates as the inter-electrode air

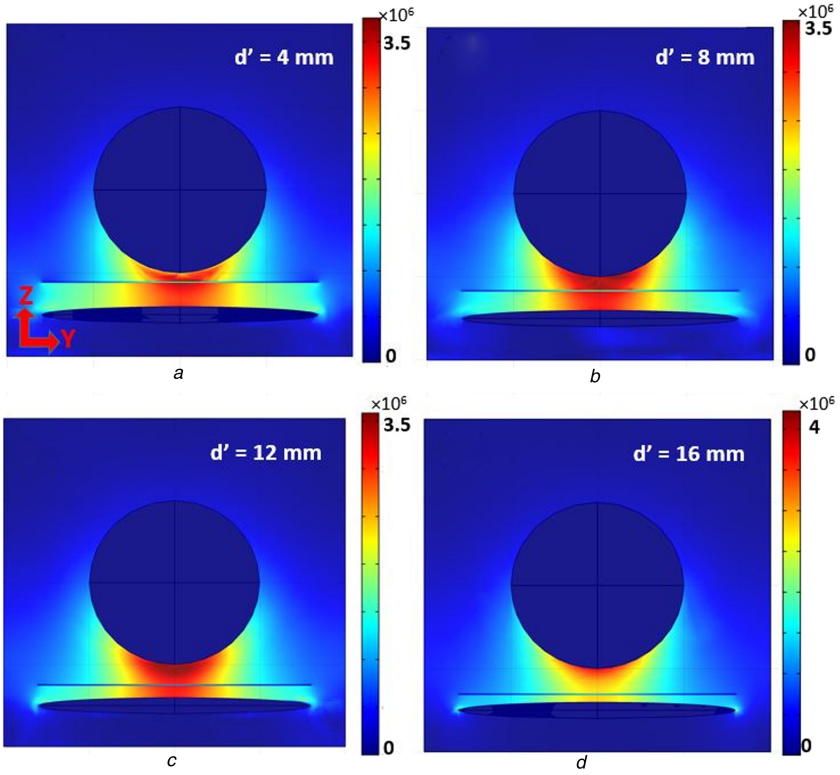


**Fig. 10** *Electric field distribution at pre-breakdown instant in sphere/plane configurations in the presence of dielectric barrier located at* ***(a)*** $d' = 5$ mm, ***(b)*** $d' = 10$ mm, ***(c)*** $d' = 15$ mm, ***(d)*** $d' = 20$ mm in a constant inter-electrode distance of $d = 20$ mm

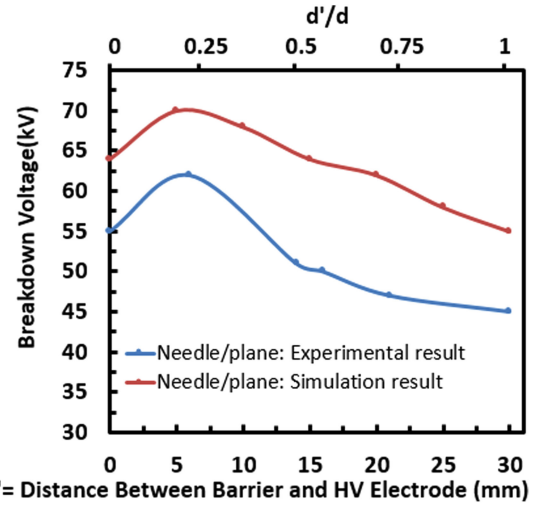


**Fig. 11** *Breakdown voltage of needle/plane arrangement under dc voltage in the presence of pressboard dielectric barrier placed at varying distances from the HV electrode, d', in a constant inter-electrode distance of d = 30 mm*

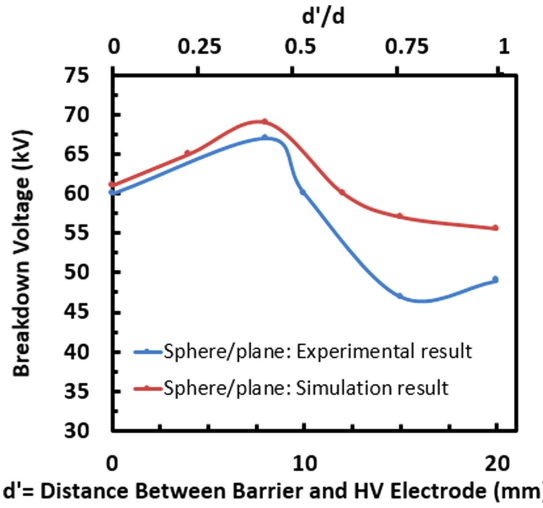


**Fig. 12** *Breakdown voltage of sphere/plane arrangement under dc voltage in the presence of a PTFE dielectric barrier placed at varying distances from the HV electrode, d', in a constant inter-electrode distance of d = 20 mm*

gap increases from 20 to 30 mm, evidenced by the reduced slope in the two lines representing electrodes with PVC heat shrinkage. This can be explained using a simple electrical model for the electrode system (see Fig. 14). In the figure, the different dielectric layers between electrodes are represented by capacitances $C_d$ and $C_g$. In addition, the element $C_s$ stands for the stray capacitance of the source. With increasing air gap, $C_g$ decreases and the voltage distribution changes, i.e. higher relative voltages are applied to the air gap and as a result breakdown may occur at relatively lower voltages.

Fig. 15 shows breakdown voltages for electrode configurations with and without a dielectric barrier under ac applied voltage. As can be seen in the figure, again, the breakdown voltage increased with an increase in inter-electrode gap distance. Also note that the breakdown voltage does not change linearly with distance. In the case of the electrode with a 0.32 mm PVC barrier, the change of breakdown voltage with respect to inter-electrode distance is much more non-linear. In other words, the impact of PVC heat shrinkage becomes less important in the case of large inter-electrode spacing, same as in the applied dc voltage case.

*4.2.1 Simulation results:* In this section, we present a method to calculate the pre-breakdown electric field distribution in the air gap and also inside the dielectric barrier using simulation models. Breakdown voltage in this case happens when the electric field inside the dielectric barrier exceeds the dielectric strength of PVC, and, consequently, the streamer criterion is met for the breakdown path between HV and ground electrodes. Immediately after that, a discharge channel is built through the barrier, providing a low impedance path from the HV electrode tip to the ground electrode. The electric field distribution in the air gap and inside the dielectric barrier was calculated by solving the model in software for the

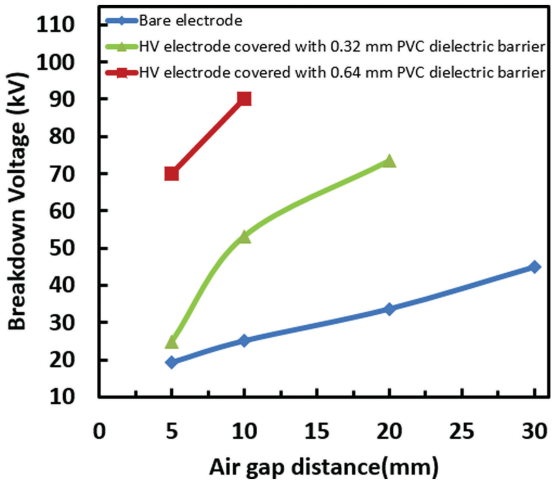


**Fig. 13** *Breakdown voltage of four U-shape/plane electrode configurations under dc voltage*

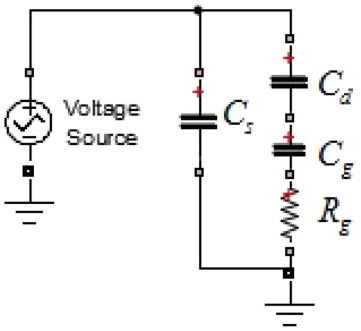


**Fig. 14** *Equivalent circuit of dielectric layers*

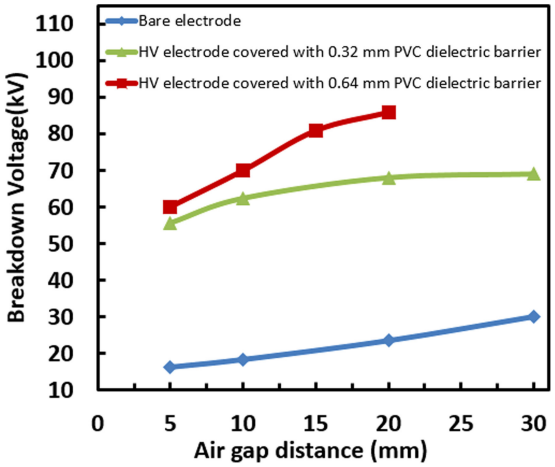


**Fig. 15** *Breakdown voltage electrode with and without barrier under ac voltage*

specific initial voltage conditions. If either of the mentioned criteria are not met, the voltage was changed to calculate the lowest voltage magnitude that satisfied all the conditions.

Fig. 16 shows the electric field along the straight line that connects the U-shape electrode to the ground electrode immediately before the breakdown voltage happens. It can be seen from the figure that the electric field has its maximum inside the dielectric barrier and decreases rapidly in the air gap. The electric field along the straight line is approximately uniform after 4 mm distance from the HV electrode. The reason is that electric charges were accumulated on the barrier surface and they produce electric field components directly opposite the applied field. Consequently, the electric field decreases in the air gap and increases in the dielectric coating.

Fig. 17 shows the top view of the electric field distribution inside the PVC in the curvature part of dielectric barrier at the pre-

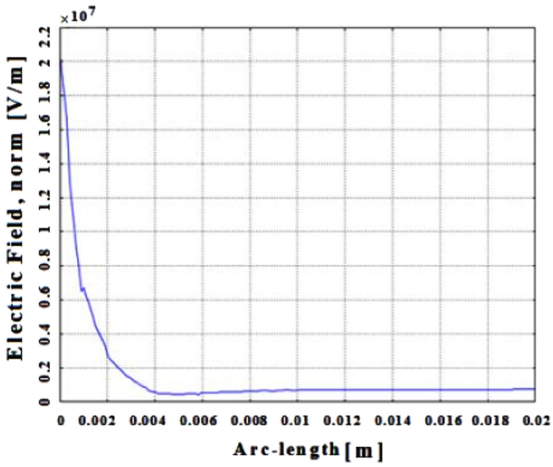


**Fig. 16** *Electric field distribution along the z-axis in U-shape/plane electrode arrangement with covered heat shrinkage PVC*

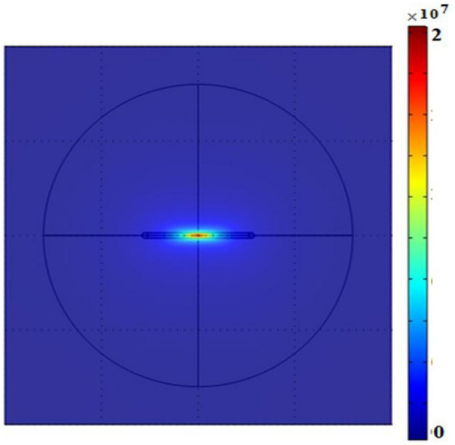

**Fig. 17** *Electric field distribution in PVC heat shrinkage*

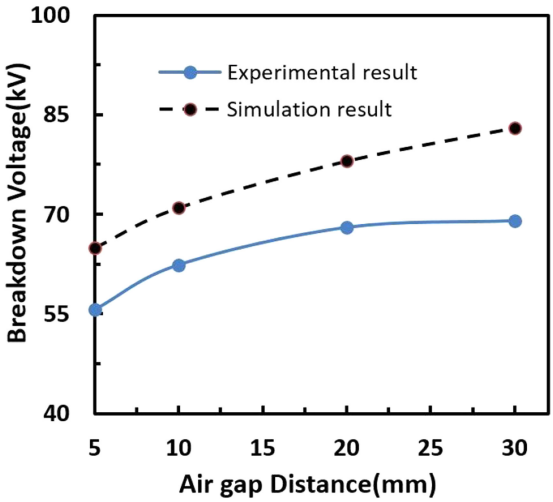


**Fig. 18** *Experimental and simulation result of breakdown voltage in U-shape/plane electrode with 0.32 mm PVC*

breakdown instant. As can be seen in Fig. 17, the maximum electric field that in the pre-breakdown instant occurs at the centre of the U-shape electrode and it is equal to the PVC dielectric strength. Fig. 18 illustrates the experimental and simulation results of the breakdown voltage for a 0.32 mm layer of the PVC dielectric barrier. The simulation results approximately align with the experimental results. The maximum deviation of 14% occurred at the 30 mm inter-electrode air gap.

## 5 Conclusions

In this paper, the effect of the polymeric and cellulose dielectric barriers on the breakdown voltage was investigated. The experimental results confirmed that the impact of the barrier is dependent on the air gap length and non-uniformity factor. Also, the results highlight the effect of physical and electrical characteristics of the dielectric barriers in the breakdown voltage enhancement. It has been shown that this effect is more noticeable when the electric field non-uniformity factor is higher. When the gap is divided by the barrier, the breakdown voltage of the gap is increased by a factor between 0.4 and 3, and the exact value of the enhancement factor depends on the non-uniformity factor of initial electric field and barrier's physical and electrical characteristics. Additionally, computer models based on finite-element method for estimating breakdown voltages in air insulating systems that include solid barriers were presented using COMSOL Multiphysics 3.3 software. We presented two methods to approximately calculate the breakdown voltage in the simulation models. Finally, we used the experimental results that were carried out in the HV laboratory to validate the simulation model. The comparison study shows that the simulation results were in good agreement with the experimental results.

## 6 References


[1] Christophorou, L.G., Olthoff, J.K., Van Brunt, R.J.: 'Sulphur hexafluoride and the electric power industry', *IEEE Electr. Insul. Mag.*, 1997, **13**, (5), pp. 20–24

[2] Blennow, H.J.M., Leijon, M.A.S., Gubanski, S.M.: 'Active high voltage insulation', *J. Electrost.*, 2002, **55**, (2), pp. 159–172

[3] Foruzan, E., Akmal, A.A., Niayesh, K.*, et al.*: 'Dielectric barrier impact on heterogeneous electric field'. 2017 IEEE Int. Conf. on Electro Information Technology (EIT)

[4] Blennow, H.J.M., Sjoberg, M.L-A.: 'Electric field reduction due to charge accumulation in a dielectric covered electrode system', *IEEE Trans. Dielectr. Electr. Insul.*, 2000, **7**, (3), pp. 340–345

[5] Blennow, H.J.M., Sjoberg, M.L.-A., Leijon, M.A.S.*, et al.*: 'Effects of charge accumulation in a dielectric covered electrode system in air'. Conf. on Electrical Insulation and Dielectric Phenomena, 1999, vol. **2**, pp. 484–487

[6] Lebedev, S.M., Gefle, O.S., Pokholkov, Y.P.: 'The barrier effect in dielectrics: the role of interfaces in the breakdown of inhomogeneous dielectrics', *IEEE Trans. Dielectr. Electr. Insul.*, 2005, **12**, (3), pp. 537–555

[7] Mauseth, F., Nysveen, A., Ildstad, E.: 'Charging of dielectric barriers in rod-plane gaps'. Proc. of the 2004 IEEE Int. Conf. on Solid Dielectrics, ICSD 2004, 2004, vol. **1**

[8] Joneidi, I.A., Majzoobi, A., Shayegani-Akmal, A.A.*, et al.*: 'Aging evaluation of silicone rubber insulators using leakage current and flashover voltage analysis', *IEEE Trans. Dielectr. Electr. Insul.*, 2013, **20**, pp. 212–220

[9] Ghassemi, M., Mohseni, H., Niayesh, K.*, et al.*: 'A detailed model for discharge initiating in argon at atmospheric pressure in presence of dielectrics barriers', *IEEE Trans. Dielectr. Electr. Insul.*, 2012, **19**, (3), pp. 865–876

[10] Ghassemi, M., Mohseni, H., Niayesh, K.*, et al.*: 'A detailed model for atmospheric pressure oxygen dielectric barrier discharges'. Conf. on Electrical Insulation and Dielectric Phenomena (CEIDP), Montreal, Canada, 14–17 October 2012

[11] Forouzan, E., Ziaee-Nezhad, M., Niayesh, K.*, et al.*: 'Experimental investigation of dielectric barrier impact on breakdown voltage enhancement of copper wire-plane electrode systems'. XVIII Int. Conf. on Gas Discharge and Their Applications, Greifswald, Germany, 5–9 September 2010

[12] Ghassemi, M., Mohseni, H., Niayesh, K.*, et al.*: 'Dielectric barrier discharge (DBD) dynamic modeling for high voltage insulation'. Electrical Insulation Conf. (EIC), Annapolis, MD, USA, 5–8 June 2011, pp. 156–161

[13] Abdel-Salam, M., Singer, H., Ahmed, A.: 'On the static behavior of dielectric barrier discharges in uniform electric fields', *J. Phys. D, Appl. Phys.*, 2001, **34**, pp. 1974–1981

[14] Foruzan, E., Vakilzadian, H.: 'The investigation of dielectric barrier impact on the breakdown voltage in high voltage systems by modeling and simulation'. 2015 IEEE Power Energy Society General Meeting, 2015

[15] Abdel-Salam, M., Singer, H., Ahmed, A.: 'Effect of the dielectric barrier on discharges in non-uniform electric fields', *J. Phys. D, Appl. Phys.*, 2001, **34**, pp. 1219–1234

[16] Vogelsang, R., Farr, T., Fröhlich, K.: 'The effect of barriers on electrical tree propagation in composite insulation materials', *IEEE Trans. Dielectr. Electr. Insul.*, 2006, **13**, (1), pp. 373–382

[17] Celestin, S., Bonaventura1, Z., Guaitella, O.*, et al.*: 'Influence of surface charges on the structure of a dielectric barrier discharge in air at atmospheric pressure: experiment and modeling', *Eur. Phys. J. Appl. Phys.*, 2009, **47**, (2), p. 22810

[18] Kumara, S., Serdyuk, Y.V., Ubanski, S.M.: 'Simulation of surface charge effect on impulse flashover characteristics of outdoor plymeric insulators', *IEEE Trans. Dielectr. Electr. Insul.*, 2010, **17**, (6), pp. 1754–1763

[19] Sarfi, V., Hemmati, V.: 'Simulation of partial discharge in closely coupled cavities embedded in solid dielectrics by finite element method'. 2014 Int. Conf. on High Voltage Engineering and Application (ICHVE), 2014, pp. 1–4. doi:10.1109/ichve.2014.7035406

[20] Sarfi, V., Hemmati, V., Arabshahi, M.M.: 'Simulation of PTC devices as fault current limiters in power systems by finite element method'. 2014 Int. Conf. on High Voltage Engineering and Application (ICHVE), 2014, pp. 1–4. doi: 10.1109/ICHVE.2014.7035503

[21] Célestin, S., Canes-Boussard, G., Guaitella, O.*, et al.*: 'Influence of the charges deposition on the spatio-temporal self-organization of steamers in a DBD', *J. Phys. D, Appl. Phys.*, 2008, **10**, pp. 1–10

[22] Serdyuk, Y.V., Gubanski, S.M.: 'Computer modeling of interaction of gas discharge plasma with solid dielectric barriers', *IEEE Trans. Dielectr. Electr. Insul.*, 2005, **12**, (4), pp. 725–735

[23] Célestin, S., Allegraud, K., Canes-Boussard, G.*, et al.*: 'Patterns of plasma filaments propagating on a dielectric surface', *IEEE Trans. Plasma Sci.*, 2008, **36**, (4), pp. 1326–1327

[24] Pedersen, A.: 'On the electrical breakdown of gaseous dielectrics-an engineering approach', *IEEE Trans. Electr. Insul.*, 1989, **24**, (5), pp. 721–739

[25] Lowke1, J.J., D'Alessandro, F.: 'Onset corona fields and electrical breakdown criteria', *J. Phys. D, Appl. Phys.*, 2003, **36**, pp. 2673–2682

[26] Petcharaks, K.: 'A contribution to the streamer breakdown criterion'. Eleventh Int. Symp. on High Voltage Engineering, (Conf. Publ. No. 467), 1999, vol. **3**

[27] Abdel-Salam, M., Turky, A.A., Hashem, A.A.: 'The onset voltage of coronas on bare and coated conductors', *J. Phys. D, Appl. Phys.*, 1998, **31**, (19), pp. 25–50

[28] Hiziroglu, H.R., Sebo, S.A.: 'Calculation of breakdown voltages of short air gaps'. Conf. on Electrical Insulation and Dielectric Phenomena, 2000, pp. 435–438

[29] Chun, S.-T.: 'Spatial and temporal evolution of a pulsed corona discharge plasma', *J. Korean Phys. Soc.*, 1998, **33**, pp. 428–433

[30] Kitamura, T., Kojima, H., Hayakawa, N.*, et al.*: 'Influence of space charge by primary and secondary streamers on breakdown mechanism under non-uniform electric field in air'. 2014 IEEE Conf. on Electrical Insulation and Dielectric Phenomena (CEIDP), 2014

[31] Punekar, G.S., Kishore, N.K., Shastry, H.S.Y.: 'Effect of non uniformity factors and assignment factors on errors in charge simulation method with point charge model', *J. Electr. Syst. Sci. Eng.*, 2008, **1**, (2), pp. 115–119